

Application of a Slotted Airfoil for UH-60A Helicopter Performance

Hyeonsoo Yeo
Raytheon ITSS

Joon W. Lim
Army/NASA Rotorcraft Division
Aeroflightdynamics Directorate (AMRDEC)
US Army Aviation and Missile Command

NASA Ames Research Center
Moffett Field, California

Abstract

Recently developed forward slotted airfoils were applied to a UH-60A helicopter, and the performance has been estimated. Baseline SC1095 and SC1094 R8 airfoil characteristics were modified based on CFD calculations of an A3c slotted airfoil to incorporate aerodynamic characteristics of a high-lifting airfoil. The slotted airfoil increases maximum thrust of the UH-60A helicopter by up to 25%, but a significant penalty is observed at C_T/σ less than 0.11. This penalty results from higher drag than the baseline airfoil at low angles of attack. A drag reduction at high Mach numbers is necessary to fully exploit the airfoil capability in the rotorcraft application. Preliminary comparison of the slotted airfoil with the wide chord blade shows that the slotted airfoil has limited advantages over the wide chord blade.

Introduction

Research on advanced rotor technology has been conducted to meet the requirements of a next generation rotorcraft. These requirements include larger payload capability, higher forward flight speed, increased range and endurance, and greater maneuverability and agility. Although there has been enormous progress in the performance of modern-day airfoils compared to the first generation airfoils, the current technology of conventional fixed geometry, single-element airfoils may not be able to meet future requirements.

A recent study on slotted airfoils (Refs. 1 and 2) received great attention due to the demonstration of their high lift capability. Two forward-slotted configurations (C106 and C210) based on the RC(6)-08 airfoil were designed and tested in the Langley 8-foot Transonic Pressure Tunnel

Presented at the American Helicopter Society Aerodynamics, Acoustics, and Test and Evaluation Technical Specialist Meeting, San Francisco, CA, January 23-25, 2002. Copyright © 2002 by the American Helicopter Society International, Inc. All rights reserved.

(TPT), and it was shown that these airfoil configurations could produce 29-61% higher maximum lift than the baseline single-element airfoil [1]. High lift is achieved by putting a slot in an airfoil to permit the passage of high-energy air from the lower surface to control the boundary layer on the upper surface [3]. The rotor test showed the potential of a high-lift helicopter using the slotted airfoils [2]. However, the drag penalty at low angles of attack was notable.

To minimize the drag increase of a slotted airfoil at low angles of attack, advanced airfoil design methodology including Navier-Stokes computational fluid dynamics (CFD) code was used [4]. The study showed that the new slat design was able to reduce drag significantly at low Mach numbers while maintaining the maximum lift. Figure 1 shows the new 15% chord slat geometry (A3c) compared to the C106 configuration. However, the drag penalty compared to the baseline single-element airfoil still prevailed at high Mach numbers.

In this study, the slotted airfoils are used for performance estimation of the UH-60A Black Hawk helicopter using CAMRAD II in order to understand their effects on performance.

Background of Slotted Airfoil Research

The forward-slotted airfoils (Configurations C106 and C210) were designed and tested in the Langley 8-foot Transonic Pressure Tunnel (TPT) to determine the two-dimensional aerodynamic characteristics [1]. The RC(6)-08 airfoil was chosen as the baseline for these slotted airfoil designs. The configuration C106 of the forward slotted RC(6)-08 airfoil is shown in Figure 1. Lift and pitching moment coefficients were determined from measurements of airfoil surface static pressure, and drag coefficients were determined from measurements of wake total and static pressures. Figure 2 shows the lift coefficients of the slotted airfoil (C106) as a function of angle of attack together with those of the baseline RC(6)-08 airfoil at a Mach number of 0.4. The baseline data

were measured in the Langley 6- by 28-inch Transonic Tunnel [5]. The maximum lift coefficient ($c_{l,max}$) of the C106 airfoil was significantly increased compared to that of the baseline airfoil. The wind tunnel test has shown that the maximum lift coefficient value of the slotted airfoil (C106) was improved over the baseline airfoil by 29 percent to 43 percent for Mach numbers of 0.37 to 0.5. However, a large drag penalty was observed for the slotted airfoils especially at low angles of attack. Figure 3 shows the drag coefficients at zero lift (c_{d_0}) of the slotted airfoil (C106) and the baseline airfoil (RC(6)-08). The c_{d_0} of the slotted airfoil was more than doubled over a wide range of Mach numbers.

The baseline RC(6)-08 and two slat configurations were also tested for dynamic stall behavior in the Compressible Dynamic Stall Facility (CDSF) at the NASA Ames Research Center [6]. The test ranged over Mach number $0.2 \leq M \leq 0.5$ and reduced frequency $0 \leq k \leq 0.10$ for angle of attack $\alpha = 10^\circ + 10^\circ \sin \omega t$. For the baseline RC(6)-08 airfoil, dynamic stall inception occurred at $\alpha = 14.0^\circ$ at $M = 0.25$ and $k = 0.05$. This stall inception occurred at lower angle of attack as Mach number increased. However, the configuration C210 showed the fully attached flow condition at $M = 0.25$ and $\alpha = 18.0^\circ$ and only slight trailing edge separation was observed even at 20° angle of attack. As Mach number increases, the flow separation appears at lower angle of attack. Nonetheless, the C210 airfoil showed no evidence of dynamic stall for the conditions tested. The configuration C106 was less effective than C210 in dynamic stall performance but still more effective than the baseline single-element airfoil.

Later, wind tunnel testing was conducted in the Langley Transonic Dynamics Tunnel (TDT) to evaluate potential benefits in rotor performance associated with slotted airfoils [2]. The baseline rotor configuration had a RC(4)-10 airfoil in the inboard region ($r/R \leq 0.8$) and a RC(6)-08 airfoil in the blade tip region ($r/R \geq 0.85$). Three multi-element airfoils were tested in both hover and forward flight: two forward slotted airfoils (C106 and C210) and an aft slotted airfoil with a 3° flap down. The slotted airfoils were selected for the blade tip region ($r/R \geq 0.85$). The slotted airfoil showed performance benefits at high thrust and high advance ratios. In general, C106 offered better performance than the other two configurations.

A study was conducted using computational fluid dynamics (CFD) technology to minimize the drag of a slotted airfoil at low angles of attack while maintaining maximum lift characteristics [4]. First, OVERFLOW calculations for the RC(6)-08 baseline airfoil and the two slotted airfoils (Configurations C106 and C210) were

compared to the wind tunnel test data. Figures 4 and 5 show the lift coefficients versus angle of attack and the lift-drag polars for the RC(8)-06 and C106 configuration respectively. The origins are offset for each Mach number to better observe the airfoil characteristics. CFD calculations were compared to the wind tunnel test data at Mach numbers of 0.4, 0.6 and 0.8. In general, the lift coefficients were well predicted by the CFD calculation for both single- and multi-element airfoils. However, there was a noticeable error in the drag prediction. Although these calculated aerodynamic characteristics did not exactly match the wind tunnel test data, the general trends were reproduced by CFD solutions. It was found in Ref. 3 that the drag increase of a slotted airfoil at low angles of attack was caused by lower surface separation on the slat.

Based on the initial correlation results, a primary goal was established to minimize the lower surface slat separation while maintaining the maximum lift of the slotted airfoil. Using the CFD code and an inverse design method, new 11%, 13%, and 15% chord slat designs were developed. The C106 slat was used as a starting shape for an inverse design. The 15% chord slat geometry (A3c) obtained from the inverse design method is compared to the C106 configuration in Figure 1. The aerodynamic characteristics of the A3c airfoil are compared to the baseline RC(6)-08 and the C106 slat airfoil at Mach numbers from 0.4 to 0.7 in Figure 6. The lift and drag values are from CFD calculations. The A3c slat design provides a significant reduction in drag at low lift coefficients. Especially at $M = 0.4$, the drag coefficient of the A3c airfoil is very close to that of the baseline single-element airfoil while maintaining the maximum lift of the C106 slotted airfoil.

Approach

The forward slotted airfoil was applied for the performance estimation of the UH-60A Black Hawk helicopter. The UH-60A utilizes two different airfoils on the main rotor blade, the SC1095 and SC1094 R8. To separately include the slat effects for the current airfoils, the differences in lift, drag, and moment between the baseline RC(6)-08 airfoil and the slotted airfoil (A3c) were calculated based on the CFD calculations for all Mach numbers and angles of attack. These incremental values were added to the SC1095 and SC1094 R8 airfoil data to simulate a UH-60A with slotted airfoils. Care must be taken in this process because the baseline airfoils, RC(6)-08 and SC1095 or SC1094 R8, have different zero lift angles of attack (α_0) and stall angles of attack (α_{st}). The equivalent angle of attack (α^m) was calculated for

each Mach number as follows:

$$\alpha^m = \frac{\alpha^b - \alpha_0^b}{\alpha_{st}^b - \alpha_0^b} (\alpha_{st}^m - \alpha_0^m) + \alpha_0^m$$

where superscripts m and b represent the modified (SC1095 or SC1094 R8) and baseline (RC(6)-08) airfoils respectively. The incremental aerodynamic coefficients were added to the UH-60A airfoils for corresponding angles of attack. The modifications have been made between -6 degree and 22 degree angle of attack at all Mach numbers. Figure 7 shows the aerodynamic characteristics of the modified SC1094 R8 airfoil based on the A3c configuration together with those of the baseline SC1094 R8 airfoil for selected Mach numbers.

Results and Discussion

The effects of the slotted airfoil on the performance of the UH-60A helicopter were evaluated using CAMRAD II [7]. The trim condition in CAMRAD II specifies the rotor thrust, rotor drag, and zero one-per-rev longitudinal and lateral flapping. The specified value of rotor drag includes fuselage drag at a given speed. The trim variables are three pilot control angles (collective, lateral, and longitudinal) and a longitudinal shaft tilt angle. Performance was calculated using nonuniform inflow with a prescribed wake geometry. Unsteady aerodynamics were included, but a dynamic stall model was not used. The SC1095 airfoil extends from the blade root to 48%R and from 84%R to the blade tip. The SC1094 R8 airfoil is placed between those two sections (48% - 84%R).

Figure 8 shows the effects of the slotted airfoil on the performance of a UH-60A helicopter. In this calculation, the existing UH-60A airfoils were replaced with the slotted airfoils to investigate the effect on forward flight performance. Three slat configurations were studied separately including 1) inboard SC1095 (20% - 48%R), 2) outboard SC1095 (84% - 100%R), and 3) SC1094 R8 (48% - 84%R). All three cases used the A3c airfoil characteristics.

Figure 8(a) shows the maximum lift-to-drag ratio with respect to the thrust level. Application of the slotted airfoil on the UH-60A helicopter resulted in a significant performance penalty at low to moderate thrust levels, but demonstrated a significant benefit at high thrust levels. Using a slat on the inboard section of a blade had little performance penalty at low to moderate thrust levels, but the performance improvement was small at high thrust levels because of the low dynamic pressure inboard. Using a slat for the SC1094 R8 airfoil appears more effective than using it for the outboard SC1095

airfoil. Although the A3c airfoil design reduced drag significantly at low Mach numbers compared to the C106 airfoil [4], the drag penalty was still dominant at high Mach numbers. Thus, the slotted SC1095 airfoil in the tip region (84% - 100%R), where the blade on the advancing side sees higher Mach numbers and lower angles of attack than inboard, experienced greater drag penalty (20% reduction of maximum lift-to-drag ratio at $C_T/\sigma = 0.06$ from the baseline).

Figure 8(b) shows the maximum thrust coefficient with respect to the advance ratio. The maximum thrust was defined as the highest thrust level where CAMRAD II could achieve a converged propulsive trim solution. Except for an advance ratio of 0.4, the modified SC1094 R8 airfoil with a slat (48% - 84%R) increases thrust by 15 to 25% compared to the baseline rotor. The modified SC1095 airfoil outboard (84% - 100%R) shows the same lifting capability as the modified SC1094 R8 airfoil at an advance ratio of 0.35 and above. The slotted SC1095 airfoil inboard (20% - 48%R) has small influence on the maximum thrust.

Load factor calculations were made at $\mu = 0.35$. For these calculations, the collective angle was progressively increased for a zero shaft angle up to and through stall. The trim solution specified zero first harmonic flapping. This approach is an approximate way of looking at maneuver capability and does not include effects of dynamic stall on lift augmentation. Figure 8(c) shows the rotor induced power plus the profile power versus rotor thrust. The equivalent rotor drag can be calculated by dividing rotor induced plus profile power by airspeed. Thus, this figure provides information equivalent to a maneuver lift-drag polar. Without stall, there is only a moderate increase in the induced+profile power as thrust is increased. As stall becomes important, then the slope of this maneuver polar quickly steepens. The modified SC1094 R8 airfoil with a slat (48% - 84%R) shows a significant reduction in power for C_T/σ beyond the 0.11. The modified SC1095 airfoil outboard (84% - 100%R) requires more power than the baseline rotor up to C_T/σ of 0.126, but shows better performance than the baseline blade for C_T/σ beyond the 0.126. The slotted SC1095 airfoil inboard (20% - 48%R) has again negligible influence on the maneuver capability.

Figure 9 shows the effect of the slotted airfoil on the required power. At C_T/σ of 0.08, slotted airfoils require more power than the baseline at all advance ratios. Using the slotted SC1094 R8 airfoil requires 4 to 6% more power and using the slotted SC1095 airfoil outboard requires 7 to 15% more power than the baseline. The benefit of using slotted airfoils occurs at C_T/σ of 0.12. Using the slotted SC1094 R8 airfoil requires less power

for the advance ratio of 0.28 or higher. The slotted SC1095 airfoil outboard reduces required power for an advance ratio of 0.33 or higher. At C_T/σ of 0.14, the slotted airfoil significantly reduces the required power and increase maximum speed. For example, the slotted airfoil reduces the required power by almost 30% at $\mu = 0.2$. Figure 10 shows the effect of the slotted airfoil on the lift-to-drag ratio. Similar to its effect on the required power, application of the slotted airfoil is effective only at high thrust levels. The slotted airfoil application gives a 5 to 8% loss of the lift-to-drag ratio for the 48% to 84%R span and a loss of 10% to 18% for the 84% to 100% span at C_T/σ of 0.08. However, up to 7% gain of the lift-to-drag ratio is observed for C_T/σ of 0.12 by replacing the slotted airfoil in the 48% to 84% span.

Figure 11 shows the angle of attack versus Mach number for the non-dimensional blade radius of 0.44, 0.62, 0.81, and 0.94 at every 15 degree azimuth angle. The dotted line shows the angle of attack at which c_l versus c_d curve of the modified airfoil meets that of the baseline airfoil. Thus, the slotted airfoil has better lift-to-drag ratio above the line. At C_T/σ of 0.08, the slotted airfoil is worse than the baseline airfoil over almost all the rotor disk. Although there is some benefit in the inboard section of the blade, the benefit seems to be very minimal due to low dynamic pressure. At C_T/σ of 0.12, the area where there is benefit of using the slotted airfoil dramatically increases. The beneficial area of using the slotted airfoil is more on the inboard section of the blade and the retreating side of the rotor disk. The slotted airfoil was focused on the increase of c_{lmax} or the delay of retreating blade stall, but there is a significant loss on the advancing side of the rotor disk, where the angle of attack generally never exceeds the stall angle of attack.

Figures 12 and 13 show the effects of the slotted airfoil on the lift and drag distribution along the blade span for an advance ratio of 0.35. The average $M^2 c_l$ and $M^2 c_d$ values for a slotted airfoil are compared to the baseline values. There is little change in the lift distribution. However, there is a sizable increase in drag at C_T/σ of 0.08 at all blade span. The drag penalty is larger in the blade tip area. A significant drag reduction by using the slotted airfoil is observed at C_T/σ of 0.12. The benefit of using slotted airfoil is shown along the span up to 92% of blade radius. The retreating side and inboard section of the blade, where the blade section experiences high angle of attack, appear to be the region where the slotted airfoil should be used. However, the benefit of using the slotted airfoil seems to be small due to low dynamic pressure at that region. This shows that there should be a significant reduction of drag at high Mach numbers.

Ideal Slotted Airfoil

An ideal slotted airfoil was generated by reducing drag at high Mach numbers to similar level as $M = 0.4$ to investigate the importance of a drag reduction at high Mach numbers. Figure 14 shows the aerodynamic characteristics of the ideal SC1094 R8 airfoil together with those of the baseline SC1094 R8 airfoil and the modified SC1094 R8 airfoil based on the A3c airfoil from $M = 0.4$ to $M = 0.7$. The SC1095 airfoil was also modified similar to SC1094 R8 airfoil and used outboard.

Figure 15 shows the maximum lift-to-drag ratio and load factor available with the ideal slotted airfoils. The maximum thrust was not shown because the drag reduction at high Mach numbers had no influence on it. The ideal slotted SC1095 airfoil outboard (84% - 100%R) increases the maximum lift-to-drag ratio dramatically at low to moderate thrust ratios and has a negligible influence at high thrust ratios. Ideal slotted SC1094 R8 airfoil (48% - 84%R) shows small improvement at low to moderate thrust ratios. The ideal slotted SC1095 airfoil outboard (84% - 100%R) significantly improves the maneuver performance at low thrust levels, thus this airfoil shows same or better performance than the baseline rotor at all thrust ranges. The ideal slotted SC1094 R8 airfoil (48% - 84%R) shows slightly better maneuver performance than the baseline slotted blade. These results show that the drag reduction at high Mach numbers is important: 1) for the reduction of performance penalty at low to moderate thrust ratios and 2) for the expansion of the slotted airfoil application for the tip area, where the dynamic pressure is high. This also shows that the drag reduction does not improve performance at high thrust ratios, where lift has a more important role than drag on the performance.

Slotted Airfoil versus Wide Chord Blade

The effects of the slotted airfoils on the performance of a rotorcraft (performance penalty at low thrust levels and benefit at high thrust levels) are considered similar to those of the wide chord blade because an increased chord should increase the profile drag but reduce the effects of stall at higher thrust levels.

Figure 16 compares the effects of a slotted airfoil with those of wide chord blades on the performance of a UH-60A helicopter. The SC1094 R8 airfoil with a slat (48%R - 84%R) was chosen for the comparison because it provided the best performance results among tested spanwise slat locations. Two wide chord planforms are used for the performance calculation: 10% increase of chord for SC1094 R8 airfoil (48%R - 84%R) and 20% increase of chord for SC1094 R8 airfoil (48%R - 84%R).

Figure 16(a) shows the maximum lift-to-drag ratio with

respect to the thrust level. The slotted airfoil and the wide chord blades show same trends. A 10% chord increase performs better than the slotted airfoil at low to moderate thrust levels, but shows lower best lift-to-drag ratios than the slotted airfoil at high thrust levels. A 20% chord increase shows very similar best lift-to-drag ratios as the slotted airfoil at low thrust levels, but perform better than the slotted airfoil at C_T/σ between 0.09 and 0.15. Figure 16(b) shows the maximum thrust coefficient with respect to the advance ratio. Both wide chord blades increase the maximum thrust compare to the baseline rotor. However, the slotted SC1094 R8 airfoil shows better thrust capability. Figures 16(c) shows the required power at C_T/σ of 0.12. Using the slotted SC1094 R8 airfoil requires less power than the baseline for the advance ratio of 0.28 or higher. Both wide chord blade planforms require less power than the slotted airfoil as well as the baseline. The power reduction of the wide chord blades range 9 to 13% at the advance ratio of 0.4. Similar trend is observed for the lift-to-drag ratio as shown in Figures 16(d). The wide chord blades increase the lift-to-drag ratio up to 22%.

Conclusions

Recently developed forward slotted airfoils were applied to a UH-60A helicopter and the performance has been estimated. Baseline SC1095 and SC1094 R8 airfoils were modified based on CFD calculations of an A3c slotted airfoil to incorporate aerodynamic characteristics of a high-lifting airfoil. The effects of the slotted airfoils on the performance of a rotorcraft were also compared with those of the wide chord blade. From this study, the following conclusions are drawn;

1. The slotted airfoil shows high lift capability. The slotted airfoil increases maximum thrust by up to 25% and maneuvering capabilities at high g 's. However, a significant penalty is shown in terms of required power and lift-to-drag ratio at C_T/σ less than 0.11.
2. Although the A3c airfoil significantly reduced the drag at low angles of attack compared to the C106 airfoil at low Mach numbers, a drag reduction at high Mach numbers is necessary to fully exploit the airfoil capability in the rotorcraft application.
3. Among tested spanwise slat locations, having SC1094 R8 airfoil with a slat (48%R - 84%R) shows best performance for the UH-60A.
4. Preliminary comparison of the slotted airfoil with the wide chord blade shows that the slotted airfoil has limited advantages over the wide chord blade.

Acknowledgment

The authors would like to express thanks to Dr. Chee Tung, AFDD at NASA Ames Research Center for his encouragement and insight for this study and to Mr. Kevin Noonan, AFDD at NASA Langley Research Center and Mr. Jim Narramore, Bell Helicopter Textron, Inc. for their sharing of valuable data and knowledge.

References

- [1] Noonan, K. W., Allison, D. O., and Stanaway, S., "Investigation of a Slotted Rotorcraft Airfoils at Mach Numbers from 0.20 to 0.88 at Full-Scale Reynolds Numbers," American Helicopter Society Aeromechanics Specialists Conference, San Francisco, California, January 1994.
- [2] Noonan, K. W., Yeager, Jr., W. T., Singleton, J. D., Wilbur, M. L., and Mirick, P. H., "Evaluation of Model Helicopter Main Rotor Blade with Slotted Airfoils at the Tip," Proceedings of the 55th Annual Forum of the American Helicopter Society, Montreal, Quebec, Canada, May 1999.
- [3] Abbott, I. H., and von Doenhoff., A. E., *Theory of Wing Sections*, Dover, New York, 1959.
- [4] Narramore, J. C., McCroskey, W. J., and Noonan, K. W., "Design and Evaluation of Multi-Element Airfoils for Rotorcraft," Proceedings of the 55th Annual Forum of the American Helicopter Society, Montreal, Quebec, Canada, May 1999.
- [5] Noonan, K. W., "Aerodynamic Characteristics of a Rotorcraft Airfoil Designed for the Tip Region of a Main Rotor Blade," NASA TM 4264, May 1991.
- [6] Carr, R. W., Chandrasekhara, M. S., Wilder, M. C., and Noonan, K. W., "Effect of Compressibility on Suppression of Dynamic Stall Using a Slotted Airfoil," *Journal of Aircraft*, Vol. 38, No. 2, March 2001.
- [7] Johnson, W., "Rotorcraft Aerodynamics Models for a Comprehensive Analysis," Proceedings of the 54th Annual Forum of the American Helicopter Society, Washington, D.C., May 1998.

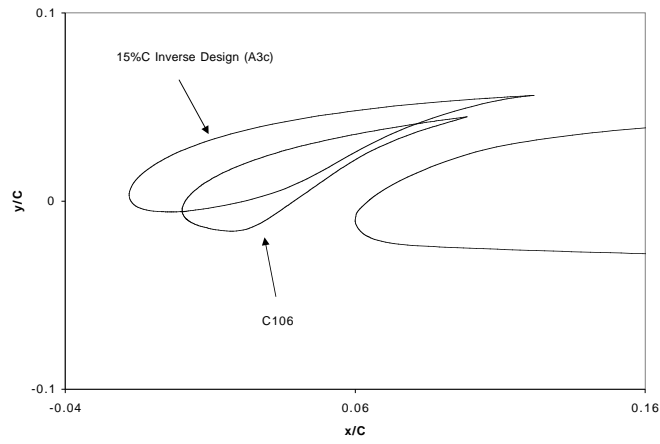


Fig. 1 C106 and A3c airfoil slat geometry [Ref. 4]

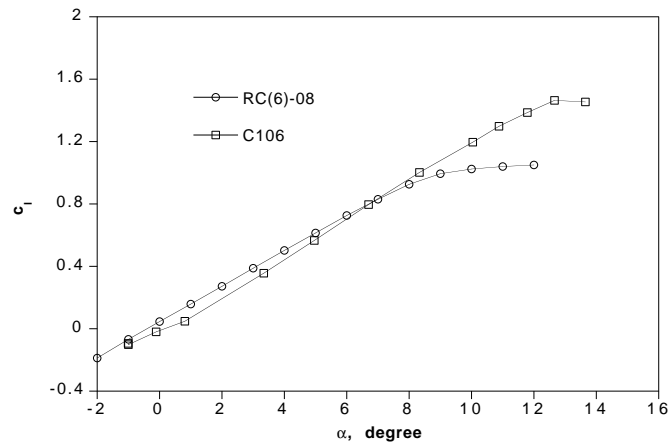


Fig. 2 Effect of slotted configuration on lift coefficients at $M = 0.4$

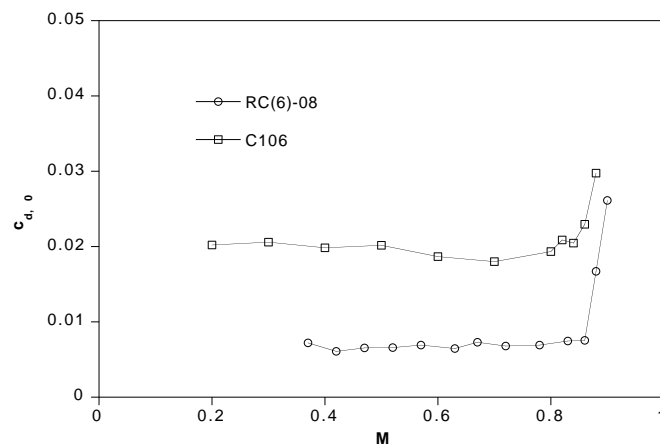


Fig. 3 Comparison of drag coefficients at zero lift angle of attack

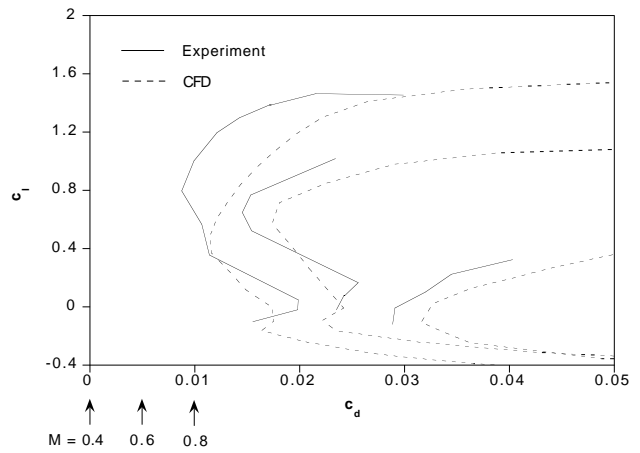
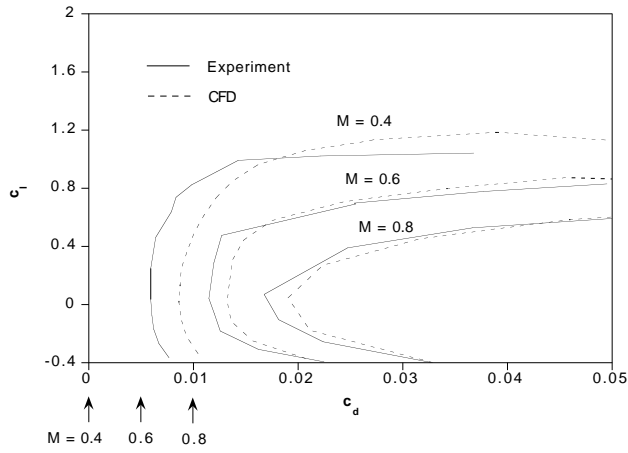
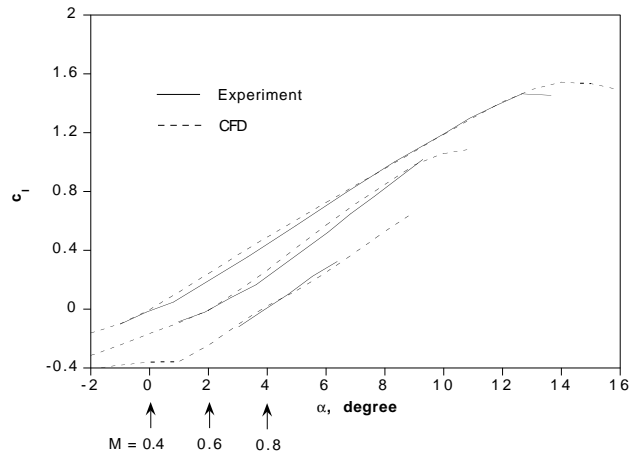
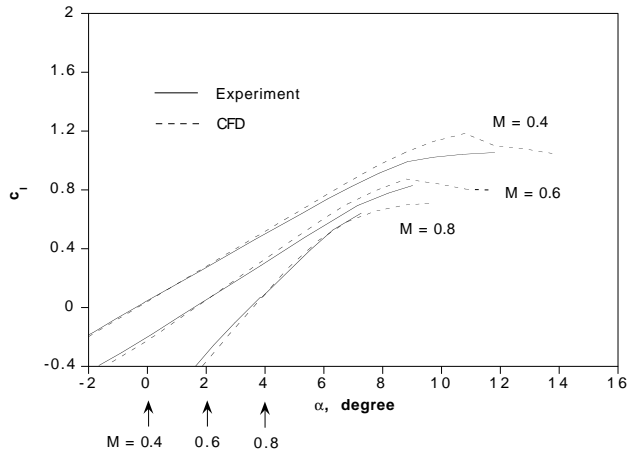
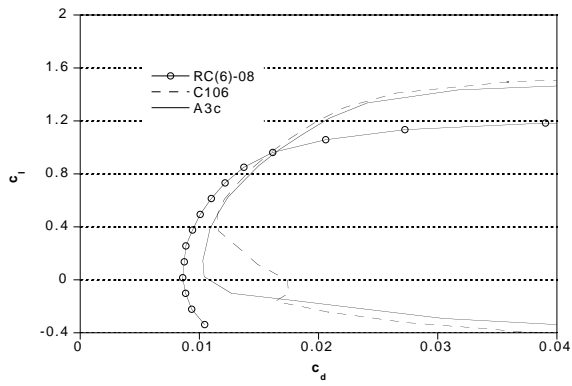
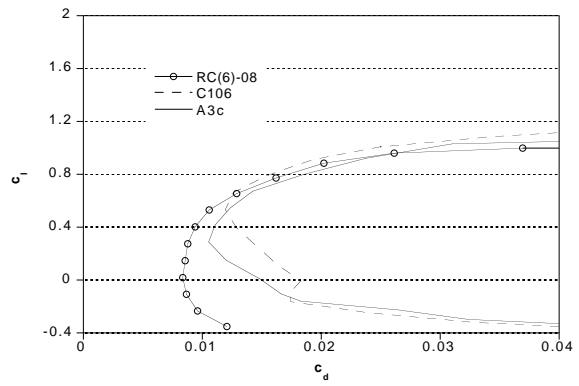


Fig. 4 Comparison of CFD results with experiment for RC(6)-08

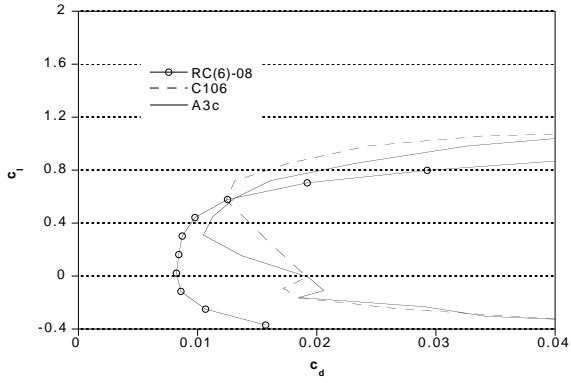
Fig. 5 Comparison of CFD results with experiment for C106



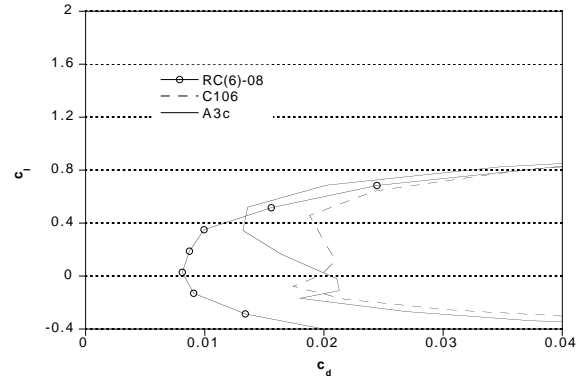
(a) $M = 0.4$



(b) $M = 0.5$

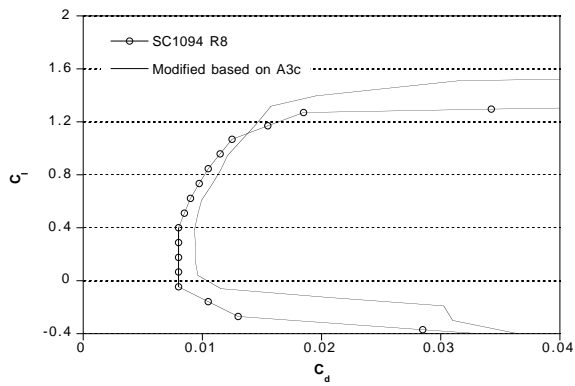


(c) $M = 0.6$

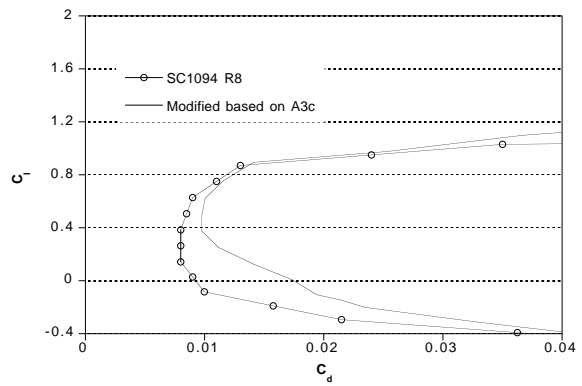


(d) $M = 0.7$

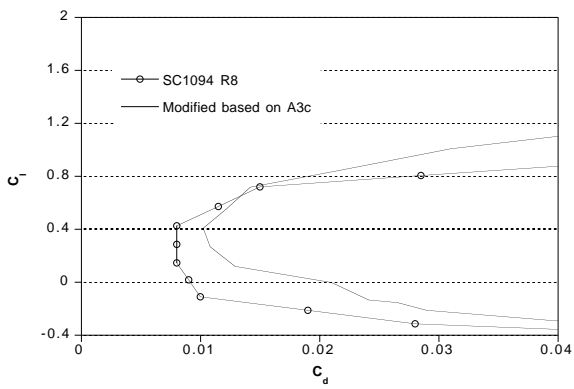
Fig. 6 Effect of slotted configurations on drag coefficient



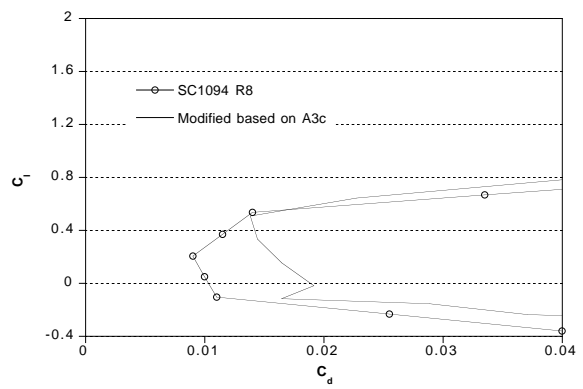
(a) $M = 0.4$



(b) $M=0.5$

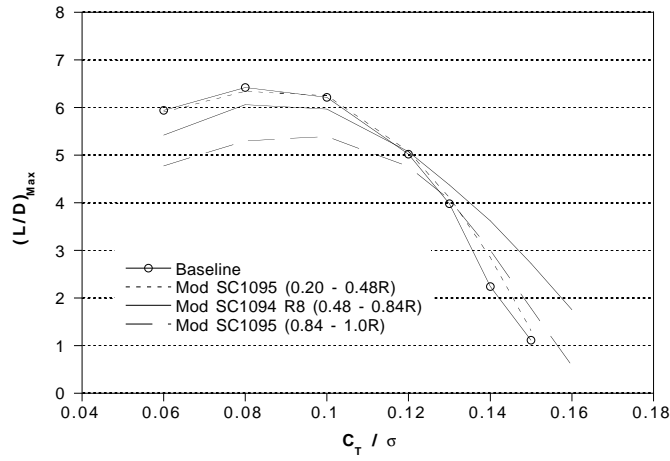


(c) $M = 0.6$

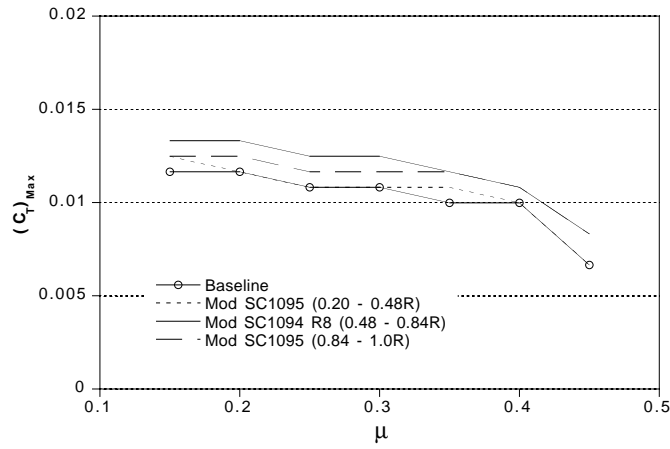


(d) $M=0.7$

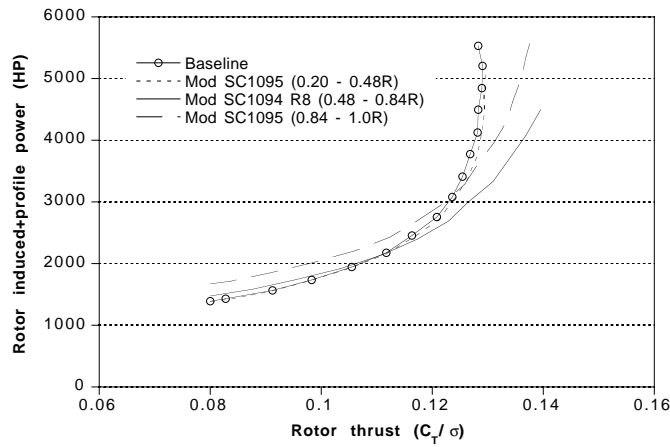
Fig. 7 c_l vs. c_d of modified SC1094 R8 airfoil



(a) Maximum lift-to-drag ratio

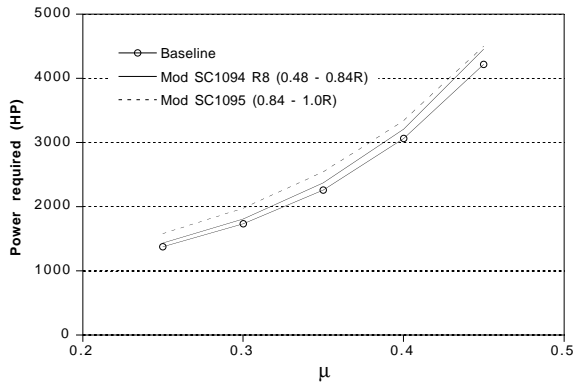


(b) Maximum thrust coefficient

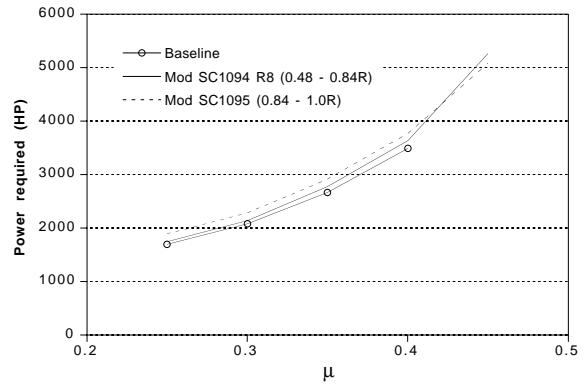


(c) Load factor available at $\mu = 0.35$

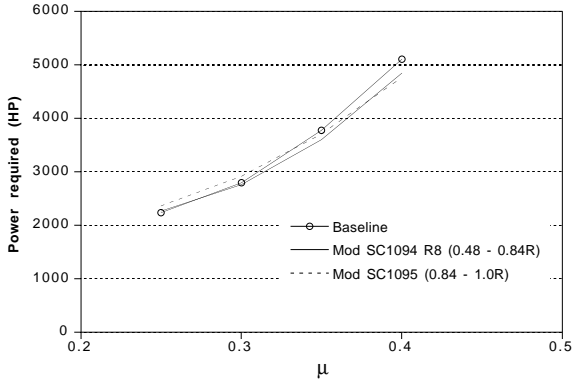
Fig. 8 Effect of slotted airfoil on performance



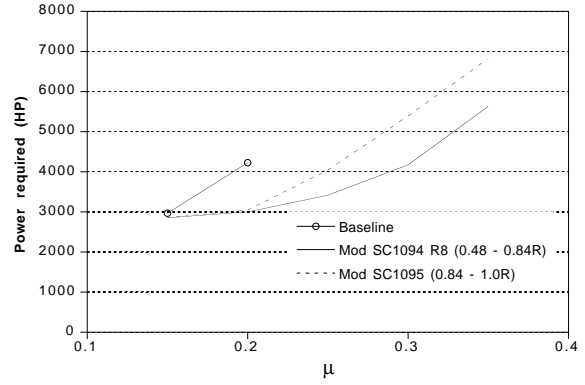
(a) $C_T/\sigma = 0.08$



(b) $C_T/\sigma = 0.10$

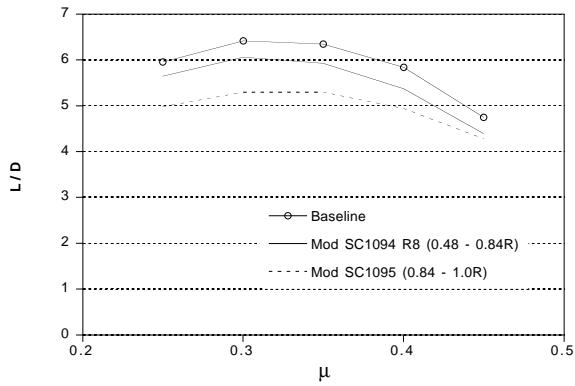


(c) $C_T/\sigma = 0.12$

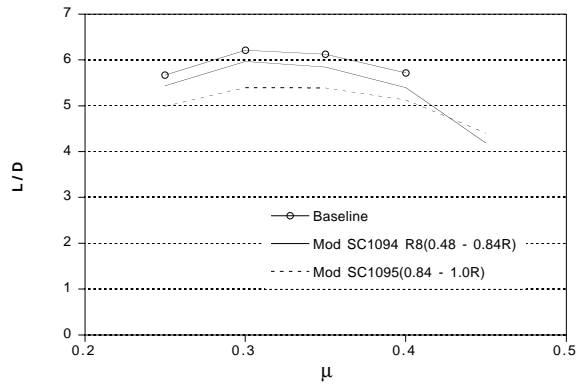


(d) $C_T/\sigma = 0.14$

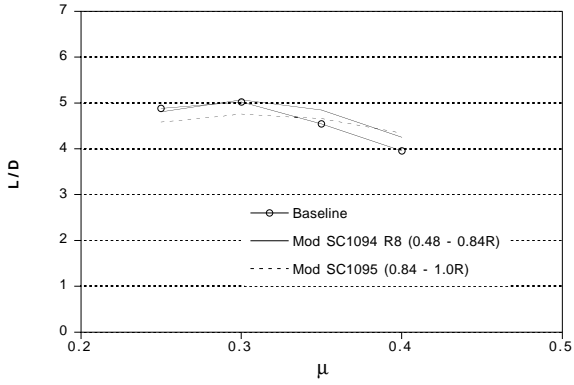
Fig. 9 Effect of slotted configurations on power required



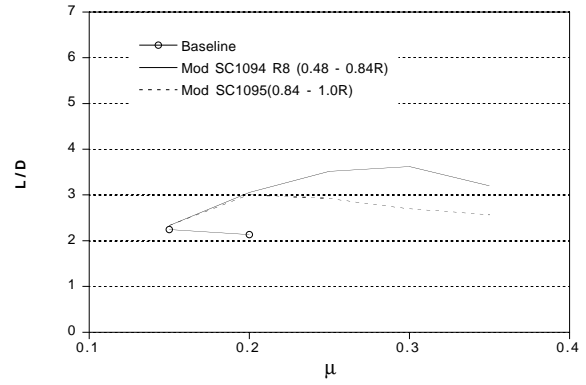
(a) $C_T/\sigma = 0.08$



(b) $C_T/\sigma = 0.10$

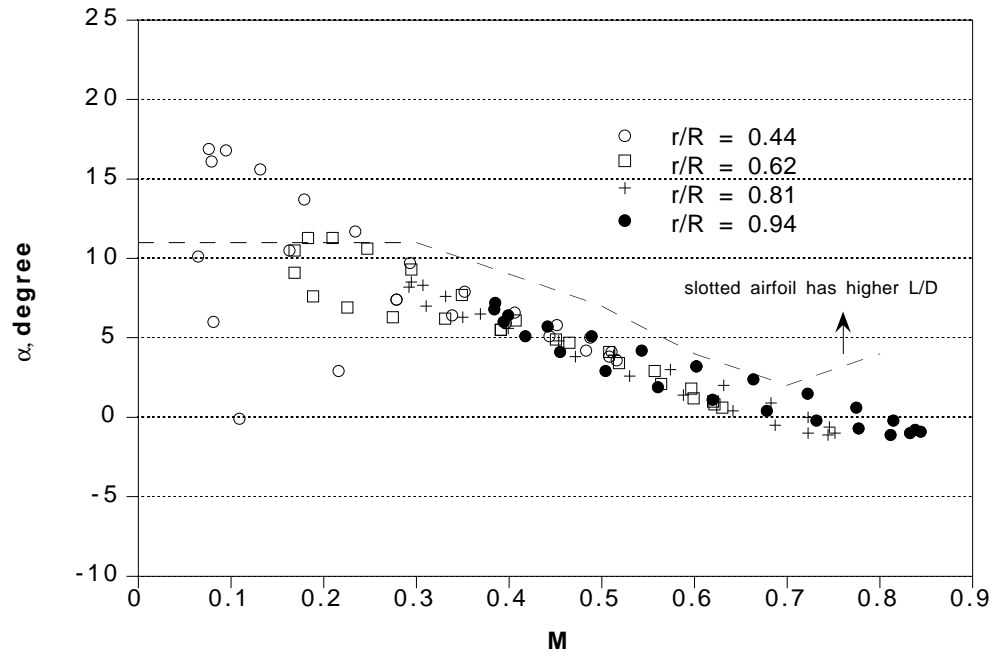


(c) $C_T/\sigma = 0.12$

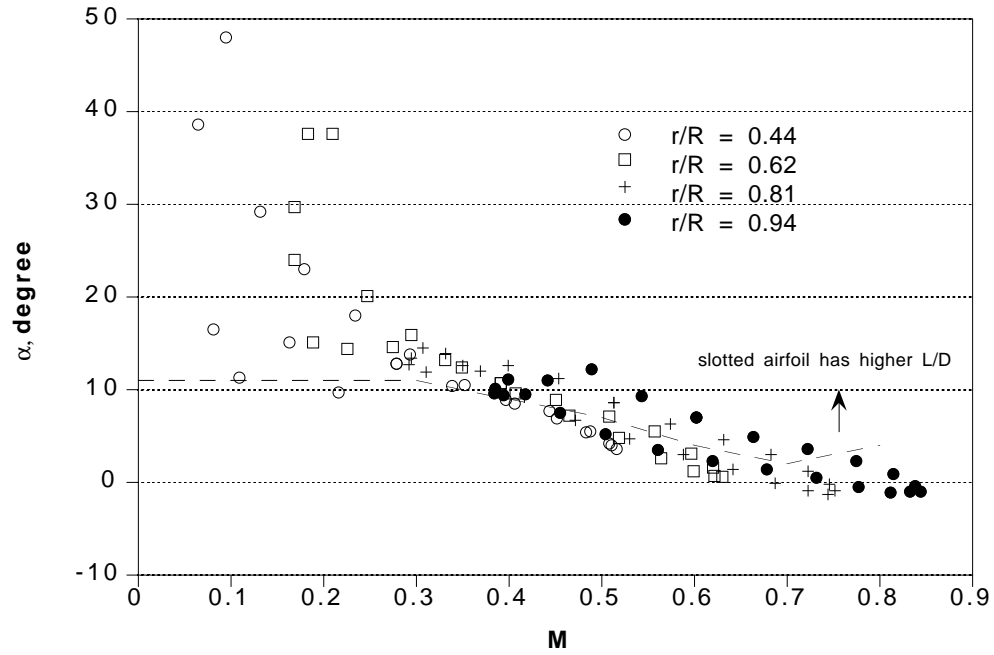


(d) $C_T/\sigma = 0.14$

Fig. 10 Effect of slotted configurations on lift-to-drag ratio

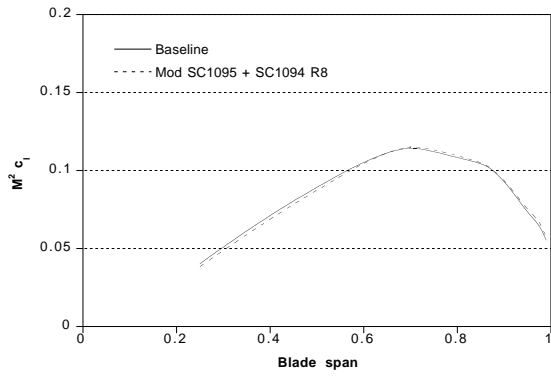


(a) $C_T/\sigma = 0.08$

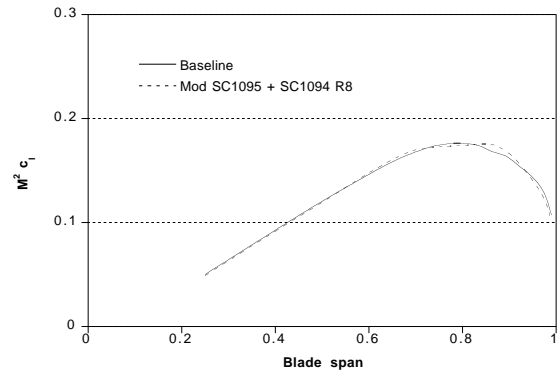


(b) $C_T/\sigma = 0.12$

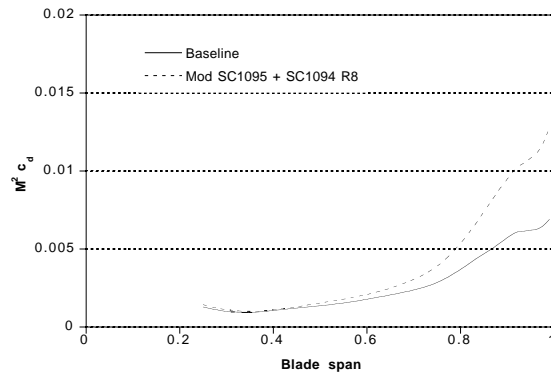
Fig. 11 Angle of attack versus Mach number, $\mu = 0.35$



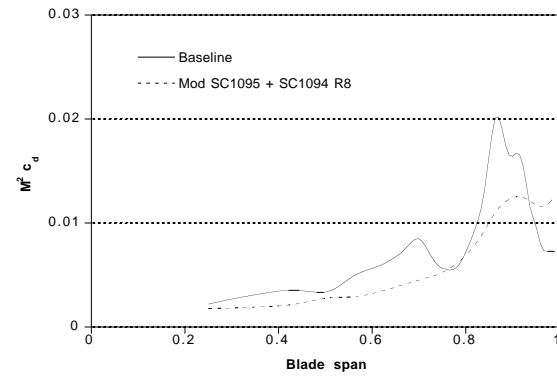
(a) $M^2 c_l$



(a) $M^2 c_l$



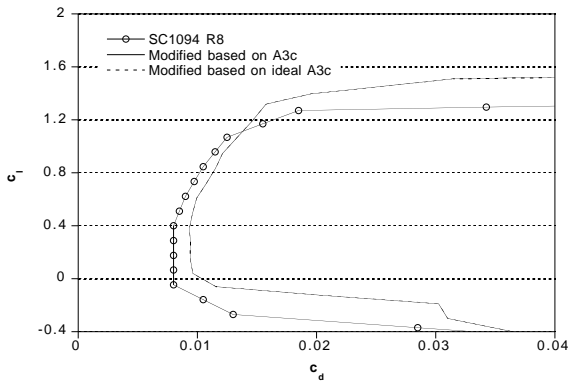
(b) $M^2 c_d$



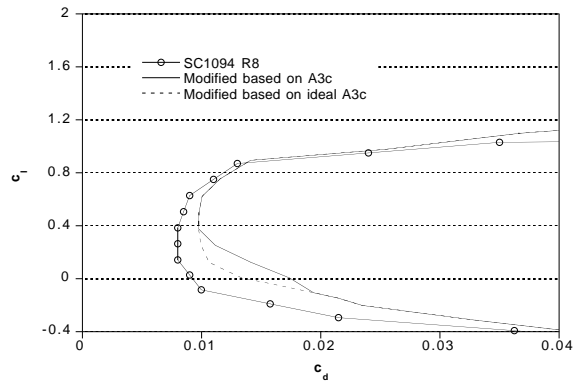
(b) $M^2 c_d$

Fig. 12 Average $M^2 c_l$ and $M^2 c_d$ distribution, $C_T/\sigma = 0.08$, $\mu = 0.35$

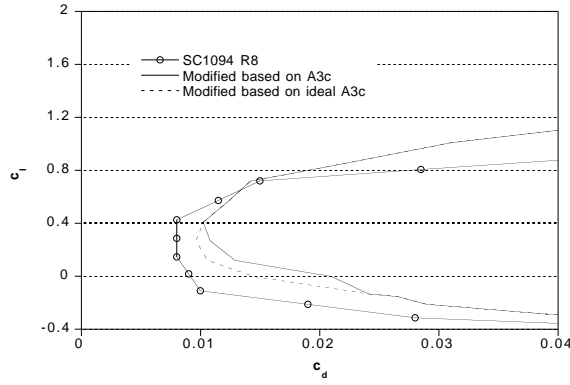
Fig. 13 Average $M^2 c_l$ and $M^2 c_d$ distribution, $C_T/\sigma = 0.12$, $\mu = 0.35$



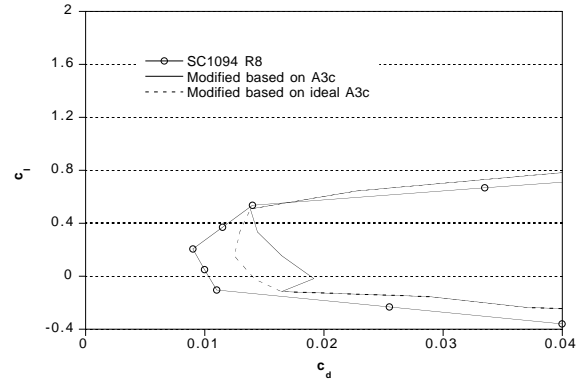
(a) $M = 0.4$



(b) $M=0.5$

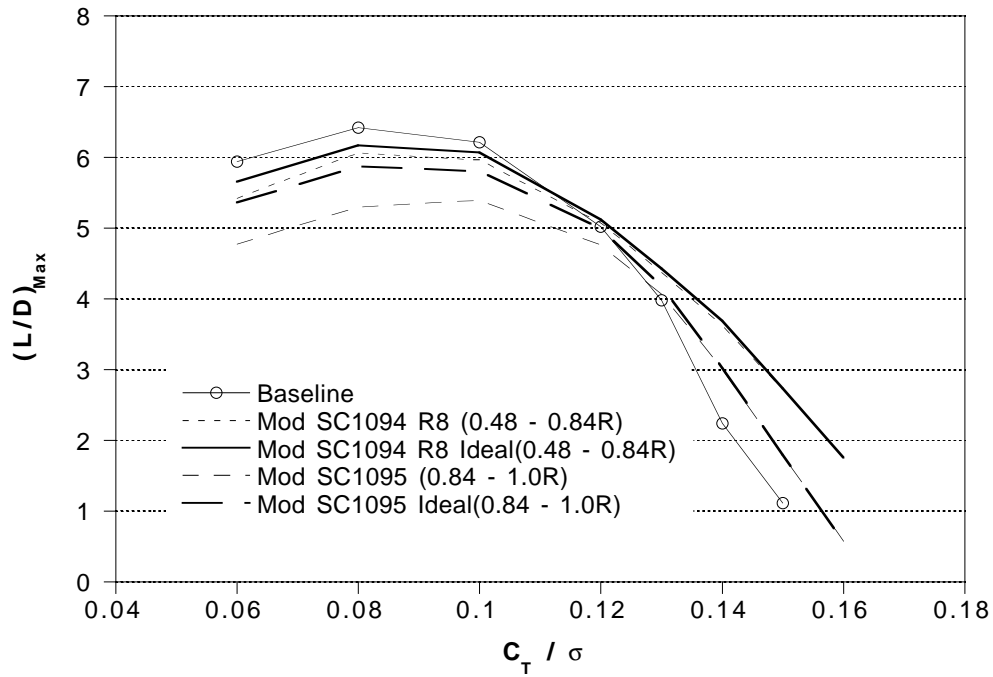


(c) $M=0.6$

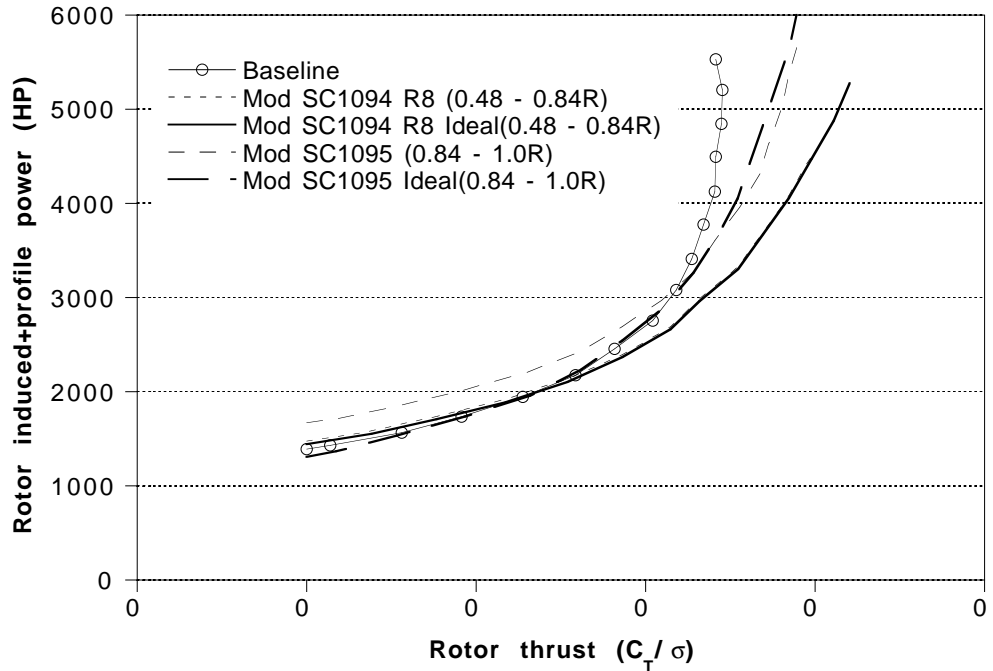


(d) $M=0.7$

Fig. 14 c_l vs. c_d for ideal slotted airfoil

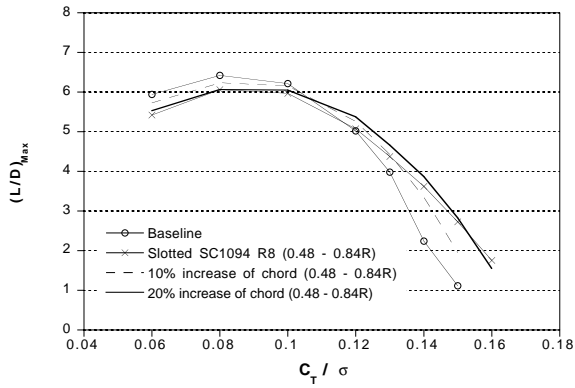


(a) Maximum lift-to-drag ratio

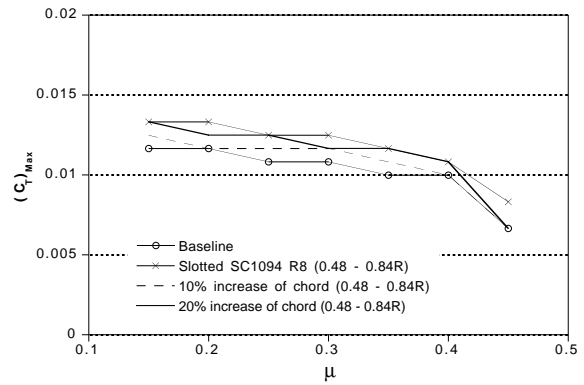


(b) Load factor available at $\mu = 0.35$

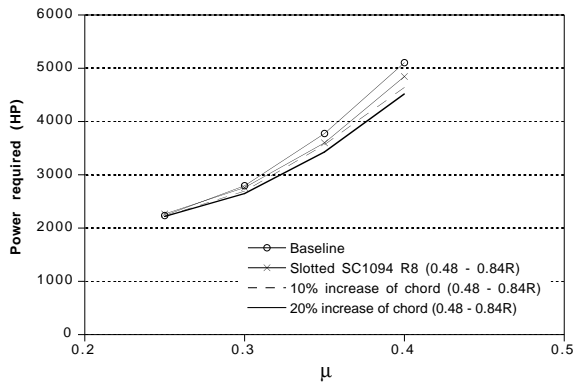
Fig. 15 Effect of ideal slotted airfoil on performance



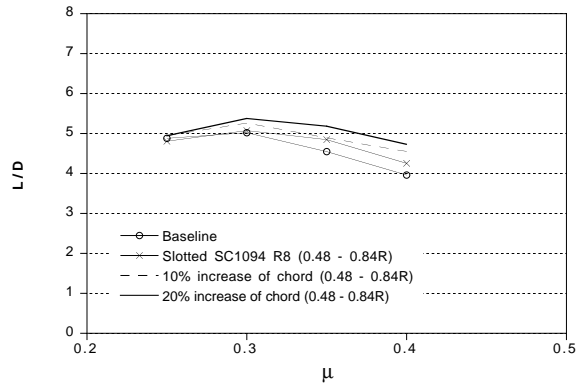
(a) Maximum lift-to-drag ratio



(b) Maximum thrust



(c) Power required at $C_T/\sigma = 0.12$



(d) Lift-to-drag ratio at $C_T/\sigma = 0.12$

Fig. 16 Comparison of slotted airfoil with wide chord on performance